Biosensors and Bioelectronics 24 (2009) 2447–2451

Contents lists available at ScienceDirect

Biosensors and Bioelectronics

journal homepage: www.elsevier.com/locate/bios

Single-crystal CeO_2 nanocubes used for the direct electron transfer and electrocatalysis of horseradish peroxidase

Xiaoling Xiao, Qingfen Luan, Xin Yao*, Kebin Zhou**

College of Chemistry and Chemical Engineering, Graduate University of Chinese Academy of Sciences, Beijing 100049, China

ARTICLE INFO

Article history:
Received 29 August 2008
Received in revised form 12 December 2008
Accepted 15 December 2008
Available online 25 December 2008

Keywords:
CeO_2 nanocubes
Direct electron transfer
Horseradish peroxidase
Chitosan
Biosensor

ABSTRACT

A new horseradish peroxidase (HRP) third-generation electrochemical biosensor based on ceria nanocubes (CeO_2-NCs) and chitosan (Chit) was developed. The single-crystalline, uniform and size-controlled CeO_2-NCs have been synthesized by hydrothermal method. HRP was immobilized in CeO_2-NCs and Chit film on the glass carbon electrode (HRP/CeO_2/Chit/GCE). Compared with HRP-chitosan modified electrode (HRP/Chit/GCE), HRP/CeO_2/Chit/GCE exhibited a pair of more obvious redox peaks at −0.348 V (versus Ag/AgCl). Experimental results indicate CeO_2-NCs greatly promoted the electron transfer between HRP and GCE. The immobilized HRP exhibited direct electrochemical behavior toward the reduction of hydrogen peroxide (H_2O_2). The resulting biosensor showed a linear range of 1–150 μM and a detection limit of 0.26 μM estimated at a signal-to-noise ratio of 3. Stability and reproducibility of the biosensor were also studied. The biological activity of HRP immobilizing in the composite film was characterized by UV–vis and FTIR spectra.

1. Introduction

Cerium oxide (ceria, CeO_2) is a rare earth oxide material from the lanthanide series. It is being used in various applications such as catalysts, fuel cells, solar cells, UV blocks, oxygen sensors, and polishing materials (Feng et al., 2006; Kim et al., 2004; Si et al., 2004; Si et al., 2005; Zhou et al., 2007). In addition, CeO_2 is noncytotoxic and has wide application in biological fields (Chen et al., 2006; Schubert et al., 2006; Tarnuzzer et al., 2005; Tsai et al., 2007). Tarnuzzer et al. (2005) found that CeO_2 nanoparticles can protect cellular damage from radiation, CeO_2 could act as effective radioprotectants for normal tissues and show a different protection in normal tissues. Schubert et al. (2006) reported that CeO_2 nanoparticles can protect nerve cells from oxidative tress and that the neruoprotection is independent of particle size. It has also been reported that free radical scavenging can be achieved by the introduction of CeO_2 nanoparticles into mammalian cells (Tsai et al., 2007). In addition, CeO_2 nanoparticles were functionalized with carboxybenzenesulfonamide and tested as inhibitors for human carbonic anhydrate (Chen et al., 2006), which have potential use for nontoxic drug delivery tool. In order to extend CeO_2 nanoparticles application, in this work it has been used to develop a new third-generation electrochemical biosensor based on the direct electron transfer of redox enzymes.

The direct electron transfer between redox proteins or enzymes and underlying electrodes is of great significance in constructing mediator-free biosensors, bioreactors and so on (Armstrong, 2002; Ashok Kumar and Chen, 2007). However, either proteins or enzymes all exhibit rather slow electron transfer rate at conventional electrodes, which may result from the deep embedding of electrochemical prosthetic groups in protein structure, unfavorable orientation and adsorptive denaturation at electrode (Li et al., 2001; Xu et al., 2007a). Therefore, many methods were used to immobilize proteins or enzymes to realize their direct electron transfer with the underlying electrodes (Ding et al., 2007; Guo and Wang, 2007; Liu et al., 2007; Xu et al., 2007b; Yan et al., 2007). As a member of the large class of peroxidases, horseradish peroxidase (HRP) has been used for construction of amperometric biosensors since it is commercially available in a highly purified form (Cai et al., 2006; Chen and Dong, 2007; Elkaoutit et al., 2008; Xu et al., 2006; Song et al., 2006; Wu et al., 2008; Xi et al., 2008; Zhu et al., 2007). In this work, the single-crystalline, uniform and size-controlled ceria nanocubes (CeO_2-NCs) have been synthesized by hydrothermal method. Then the CeO_2-NCs were used to realize the direct electron transfer of HRP by immobilizing HRP on chitosan-CeO_2 film, thus a new third-generation electrochemical biosensor of HRP was obtained. Chit was applied to many biological fields due to its excellent biocompatibility, nontoxicity, and high mechanical strength. In this system, chit was used to increase film adherence and prevent the leakage of HRP on the basis of its chemical inertness, high hydrophilicity and good film-forming ability (Feng et al., 2006; Huang et al., 2002).

* Corresponding author. Tel.: +86 10 88256414; fax: +86 10 88256092.
** Corresponding author. Tel.: +86 10 88256677; fax: +86 10 88256092.
E-mail addresses: yaox@gucas.ac.cn (X. Yao), kbzhou@gucas.ac.cn (K. Zhou).

0956-5663/$ – see front matter © 2008 Elsevier B.V. All rights reserved.
doi:10.1016/j.bios.2008.12.020

2. Experimental

2.1. Materials and reagents

HRP (240 U mg^{-1}) was purchased from Dingguo Bioengineering Company (Beijing). Stock solution of 15 mg mL^{-1} HRP was prepared by directly dissolving HRP in 0.05 M phosphate buffer solution (PBS, pH 7.0) and stored at 4 °C. Chitosan (Chit, from crab shells, minimum 85% deacetylated) were purchased from Sigma and were used without further purification. $Ce(NO_3)_3{\cdot}6H_2O$, NaOH and H_2O_2 (30%) solution were purchased from Beijing Chemical Reagent. Chitosan solution (3.0 mg mL^{-1}) was prepared by dissolving 3 mg chitosan in 1 mL 0.02 mol L^{-1} acetic acid. Phosphate buffer solution (PBS, 0.05 M, pH 7.0) was used as the supporting electrolyte. All chemicals were analytical grade. All solutions were made up with double distilled water.

2.2. Preparation of HRP/CeO_2/Chit/GCE

The CeO_2 suspension (3 mg mL^{-1}) was prepared by dispersing CeO_2 nanocubes in deionized water with stirring overnight. To obtain the best CV responses, the ratio of HRP/CeO_2/Chit has been optimized. Finally, the mixing solution of 5 mg mL^{-1} HRP, 1 mg mL^{-1} CeO_2 and 1 mg mL^{-1} Chit was used to prepare the HRP/CeO_2/Chit/GCE.

Before each experiment, glassy carbon electrode was polished with 1, 0.3, 0.05 μm alumina powder on a polishing cloth. Then the electrode was successively sonicated in ethanol and double distilled water. After the electrode dried by N_2, 5 μL HRP-CeO_2-Chit dispersion was dropped on the pretreated GCE surface. The electrode was left in a glass bottle in air until dry, thus the HRP/CeO_2/Chit/GCE was obtained. The HRP/Chit/GCE was prepared by dropping 5 μL HRP-Chit solution on the GCE surface.

2.3. Apparatus and measurements

Electrochemical experiments were performed on a CHI 440 electrochemical station (CH Instruments, China) with a conventional three-electrode system. The glass carbon electrode with modified film acted as the working electrode. The Ag/AgCl (saturated KCl) was used as the reference electrode and the Pt wire acted as the counter electrode. Prior to a series of electrochemical experiments, buffers were purged with highly purified nitrogen for at least 40 min and N_2 environment was kept in the whole experiment process. X-ray diffraction data were collected on MSAL-XD2 using Cu K_α radiation. The transmission electron microscopy (TEM) images were obtained with Hitachi model H-800 transmission electron microscope. UV–vis experiments were performed with UV-1102 spectrophotometer. FTIR spectra were collected on Avatar 360 FT-IR ESP.

3. Results and discussion

3.1. Characterization of CeO_2-NCs

CeO_2 nanocubes were prepared as the method reported previously (Yang et al., 2007) with some modifications. In brief, 1 g $Ce(NO_3)_3{\cdot}6H_2O$ was reacted with proper amount 10% NaOH for about 30 min with stirring. Then all products were transferred into a 50 mL autoclave, in which the final NaOH concentration was about 8 M, the total volume was 80% of the autoclave. After heated at 180 °C for 15 h, the system was then allowed to cool to room temperature. The precipitate was filtrated, then washed with deionized water to remove the ionic remnants and then dried at 60 °C. After that the single-crystalline, uniform and size-controlled CeO_2 nanocubes were obtained. The size and morphology of the as-synthesized products were examined by TEM and shown in Fig. 1(inset). The as-obtained CeO_2 nanocubes exhibit regular cubic shapes and the mean size is about 100 nm. The X-ray diffraction pattern of CeO_2 nanocubes (Fig. 1) indicates that all peaks can be indexed to the pure fluorite cubic structures (space group *Fm*3*m* (225), JCPDS 34-0394).

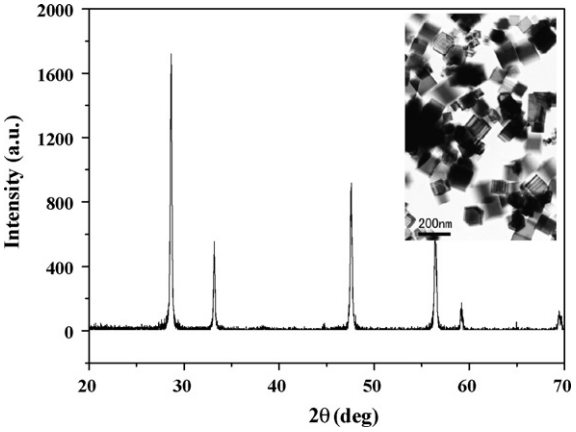

Fig. 1. X-ray diffraction pattern of CeO_2-NCs. Inset: TEM micrographs of CeO_2-NCs.

3.2. Spectroscopic analysis of HRP-CeO_2-Chit hybrid film

Since the location of the UV–vis Soret absorption band of iron provides structural information about possible denaturation of heme proteins, especially conformational change in the heme group region (Kristinsson, 2002; Zhu et al., 2002), UV–vis was used to probe the structure change for heme proteins. UV–vis spectra of HRP film (curve a) and HRP-CeO_2-Chit hybrid film (curve b) casting on quartz glass slides gave Soret bands at 403 nm (Fig. 2). The Soret band of HRP entrapped in the HRP-CeO_2-Chit hybrid film almost was same with HRP film. The result indicated that HRP entrapped in HRP-CeO_2-Chit composite film had a secondary structure similar to native state of HRP in dry films, and the system based on CeO_2-Chit did not denature HRP and had good biocompatibility for HRP.

FTIR spectroscopy is another effective mean to probe into the secondary structure of proteins. The amide I band (1700–1600 cm^{-1}) and amide II band (1620–1500 cm^{-1}) correspond to C=O stretching vibration of peptide linkages and N–H bending and C–N stretching vibration in the backbone of protein, respectively (Xu et al., 2006). The FTIR spectra of HRP- CeO_2-Chit film (a), HRP film (b) and CeO_2-Chit film (c) were shown in Fig. 3.

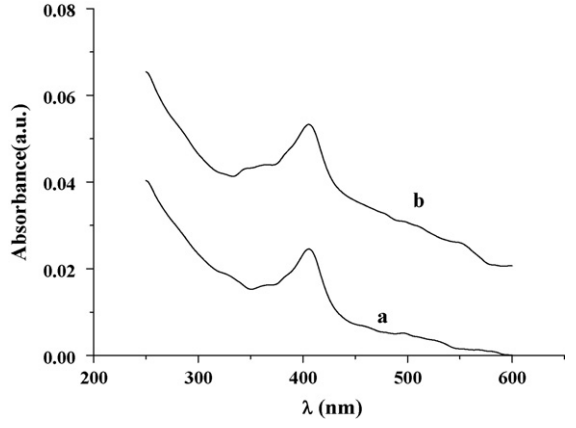

Fig. 2. UV–vis absorption spectra of HRP film (a) and HRP-CeO_2-Chit film (b).

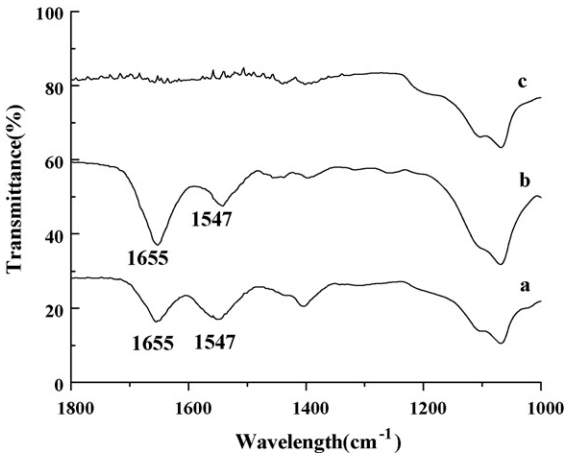

Fig. 3. FTIR spectra of HRP-CeO_2-Chit film (a), HRP film (b) and CeO_2-Chit film (c).

In our system, the spectra of amide I and II bands (1655 and 1547 cm^{-1}) of HRP in HRP-CeO_2-Chit composite film were nearly the same as those obtained for native HRP film. Just as the results of UV–vis Soret absorption, FTIR spectroscopy also proved that the structure of HRP kept almost unchanged in CeO_2-Chit film.

3.3. Direct electrochemistry of HRP/CeO_2/Chit/GCE

Fig. 4 shows the typical cyclic voltammagrams of HRP/Chit/GCE (curve a) and HRP/CeO_2/Chit/GCE (curve b) in PBS at 100 mV/s. A pair of well-defined peaks was observed for the HRP/CeO_2/Chit/GCE (curve b), corresponding to the electrochemical redox reaction between HRP-Fe(III) and HRP-Fe(II). The formal potential E^0 (defined as the average of the reduction and oxidation peak potentials) was −0.348 V, which was similar to previously reported (Liu and Hu, 2003; Sun et al., 2004). The reduction and oxidation peak potentials were, respectively, −0.367 and −0.332 V with small peak potential separation (ΔE_p = 35 mV), revealing a fast electron transfer process. The HRP/Chit/GCE also exhibited a pair of peaks, but they were much smaller. The CeO_2-CHT film inhibited the adsorption of HRP on the bare electrode and protected it from denaturation. At the same time, CeO_2 nanocubes can allow the enzyme molecules greater access to a conducting surface to favor electron transport. So the CeO_2-CHT film provided a favorable microenvironment for HRP to exchange electron with the electrode, in turn, enhanced the rate of electron transportation.

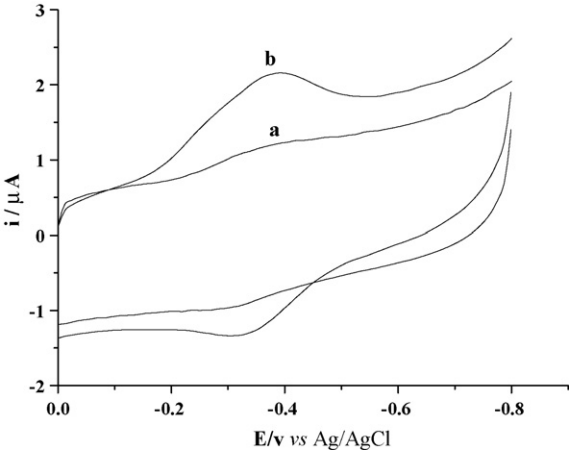

Fig. 4. Cyclic voltammograms of HRP/Chit/GCE (a) and HRP/CeO_2/Chit/GCE (b) in 0.05 M PBS (pH 7.0) solution at scan rate 100 mV/s.

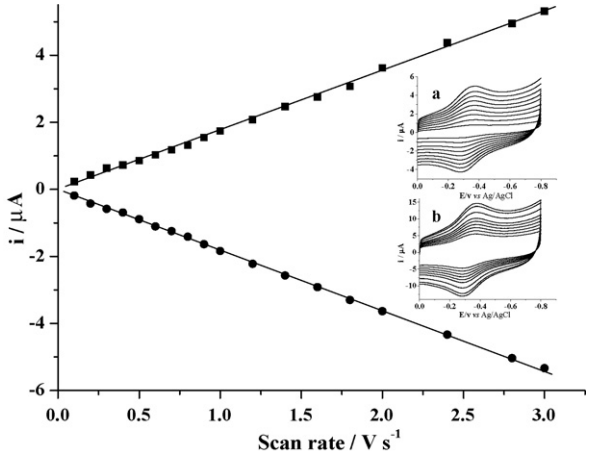

Fig. 5. Plots of oxidation peak current (●) and reduction peak current (■) versus scan rate for HRP/CeO_2/Chit/GCE. Inset shows cyclic voltammograms of HRP/CeO_2/Chit/GCE at different scan rate from 100 to 900 mV/s (a) and 1000–3000 mV/s (b) in 0.05 M PBS (pH 7.0) solution.

The surface concentration of the electroactive HRP (Γ^*) on HRP/CeO_2/Chit/GCE was estimated to be 7.06×10^{-11} mol cm^{-2} from integration of the anodic peaks according to formula (Bard and Faulkner, 1980), $Q = nFA\Gamma^*$, where A is the electrode area, n is the number of electrons transferred, and F is the Faraday's constant. The Γ^* obtained in the present work was about 3.5 times higher than that of the theoretical monolayer coverage (2×10^{-11} mol cm^{-2}) of HRP, indicating that multi-layers of HRP immobilized in the CeO_2 NCs-Chit film participated in the electron transfer process. The percentage of electroactive HRP on the electrode surface is ca. 0.7%, which is more than three times higher than the reported value (0.2%) (Huang et al., 2002). Just like former description, the CeO_2-CHT film provided a favorable microenvironment for HRP to exchange electron with the electrode, in turn, enhanced the amount of HRP participating in the electron transportation. This result also indicates that only the protein molecules close to the GCE surface and with appropriate orientation can exchange electrons with the underlying electrode (Wang et al., 2005).

Insets (a) and (b) in Fig. 5 show the cyclic voltammograms of HRP/CeO_2/Chit/GCE scanned at low scan and high scan rates, respectively. It could be seen peak currents increased with increasing scan rate from 0.05 to 3 V/s (Fig. 5), which suggested a surface-controlled process (Murray, 1984). The correlation coefficient was very close to the theoretical slope of 1 for thin layer voltammetry (Murray, 1984), which suggested that almost all electroactive HRP-Fe(III) in the film has been converted to HRP-Fe(II) on the reverse scan. Thus, HRP immobilized in CeO_2-Chit film underwent a reversible, fast and surface-controlled electron transfer. Those results indicated that CeO_2-Chit system provided a friendly microenvironment for HRP to maintain its activity to a great extent.

3.4. Electrocatalysis of HRP/CeO_2/Chit/GCE

In order to test the activity of HRP immobilized on GC by CeO_2-Chit film, its response to the reduction of H_2O_2 was examined. As shown in Fig. 6, the reduction peak linearly increased with the increase of H_2O_2 concentration, which accompanied by the decrease and disappearance of the oxidation peak (curves b–d). The linear relationship between the electrocatalytic current (i_{cat}) and the concentration of H_2O_2 using HRP/CeO_2/Chit/GCE was observed in inset of Fig. 6. Here the i_{cat} value was defined as the difference between i_{pc} in the presence of H_2O_2 and i_{pc} in the absence of H_2O_2 for the HRP/CeO_2/Chit/GCE (Liu et al., 2005). The correlation regression coefficient was 0.994 from 1 to 150 μM, and the

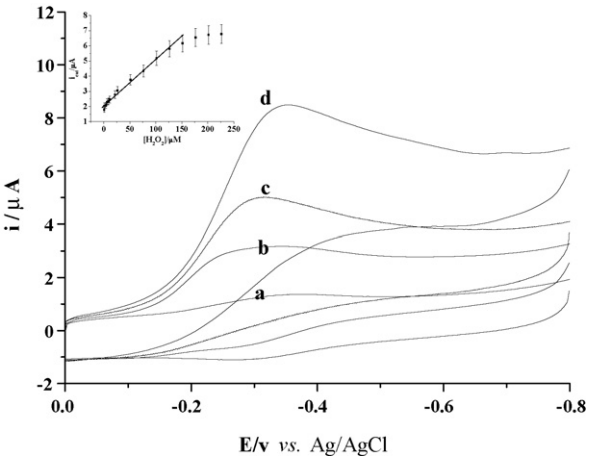

Fig. 6. Cyclic voltammograms of HRP/CeO_2/Chit/GCE in 0.05 M PBS (pH 7.0) solution with H_2O_2 concentration at (a) 0, (b) 27.5, (c) 52.5, and (d) 102.5 μM. Inset: plot of the electrocatalytic current (i_{cat}) versus H_2O_2 concentration for HRP/CeO_2/Chit/GCE in 0.05 M PBS (pH 7.0). Scan rate: 100 mV/s.

lowest detection limit was 0.26 μM at S/N = 3. The linear calibration range of H_2O_2 at HRP/CeO_2/Chit/GCE extent up to 150 μM, higher than 107 μM based on the direct electrochemical behavior of HRP immobilized on a gelatin-hydrophobic ionic liquid gel films (Yan et al., 2007) and 73 μM based on immobilized in a zirconia enhanced grafted collagen trihelix scaffold (Zong et al., 2006). The detection limit of 0.26 μM, which is a little lower than that of 0.5 μM reported in Ref (Xu et al., 2007b) and much lower than that of 1.7 μM at HRP-toluidine blue-MWNTs nanocomposite (Liu et al., 2008), and 12.89 μM of HRP immobilized in sol–gel-derived ceramic-carbon nanotube nanocomposite film (Chen and Dong, 2007) and 9.0 μM of HRP based on clay-chitosan-gold nanoparticle nanocomposite (Zhao et al., 2008).

The calibration curve of the sensor for H_2O_2 (inset of Fig. 6) exhibited a typical characteristic of Michaelis–Menten kinetics at high concentrations (when the concentration of H_2O_2 is above 150 μM, the peak current tends to stable). The apparent Michaelis–Menten constant, which gives an indication of the enzyme-substrate kinetics, could be obtained from the electrochemical version of the Lineweaver–Burk equation (Kamin and Willson, 1980):

$$\frac{I}{I_{ss}} = \frac{I}{I_{max}} + \frac{K_m}{I_{max}c}$$

where I_{ss} is the catalytic current, c is the bulk concentration of the substrate, I_{max} is the maximum catalytic current under saturated substrate conditions, and K_m is Michaelis constant. The K_m value is estimated to be 7.4×10^{-5} M, based on the slope and the intercept of the $1/I_{ss}$ versus $1/c$ plot, which was much smaller than that of the previous reports (Li et al., 2008; Zhang et al., 2008; Zhao et al., 2008). The small K_m indicates that the immobilized HRP has higher enzymatic activity, and that the biosensor has greater affinity and catalytic performance towards H_2O_2.

3.5. Stability and reproducibility of HRP/CeO_2/Chit/GCE

The stability and reproducibility of HRP/CeO_2/CHT electrode were examined by CV. The CV peak current of HRP/CeO_2/CHT electrode only decreases by 8.18% after successively scanning for 50 cycles. When the modified electrode underwent eight cycles in PBS containing 150 μM H_2O_2, the relative standard deviation of peak current is 9.05%. So the HRP/CeO_2/CHT electrode exhibited excellent stability. In addition, the reproducibility of different electrodes was also studied. Three glass carbon electrodes were modified and their difference was only 11.23%, which indicated that the reproducibility of HRP/CeO_2/CHT modified electrode was satisfied. These results demonstrated that the CeO_2 and CHT hybrid film was suitable matrix for immobilization of HRP to retain its activity and prevent it from leaking out of the film.

4. Conclusion

A novel, sensitive, reproducible and stable third-generation electrochemical biosensor of HRP was developed, which is based on the direct electron transfer between HRP and the underlying glass carbon electrode. UV–vis and FTIR spectra showed secondary structure of HRP in CeO_2-Chit film was retained. The obvious increase in peak currents of HRP/CeO_2/Chit/GCE could be attributed to the CeO_2-NCs greatly facilitating the electron transfer between the HRP and GC and it can also provide a friendly microenvironment for the immobilized HRP. Furthermore, the immobilized HRP remains its bioelectroanalytical activity to reduction of H_2O_2 with a lower detection limit and a wider liner range.

Acknowledgements

We greatly thank Prof. Zhongbo Hu for his help and discussion.

This work was supported by grants from the Ministry of Science and Technology of China (973 program no. 2006CB705601) and the National Natural Science Foundation of China (no. 20705038).

References

Armstrong, F.A., 2002. J. Chem. Soc.-Dalton Trans. 5, 661–671.
Ashok Kumar, S., Chen, S.M., 2007. Biosens. Bioelectron. 22, 3042–3050.
Bard, A.J., Faulkner, L.R., 1980. Electrochemical Methods. Wiley, New York.
Cai, W.Y., Xu, Q., Zhao, X.N., Zhu, J.H., Chen, H.Y., 2006. Chem. Mater. 18, 279–284.
Chen, H.J., Dong, S.J., 2007. Biosens. Bioelectron. 22, 1811–1815.
Chen, J.P., Patil, S., Seal, S., McGinnis, J.F., 2006. Nat. Nanotechnol. 1, 142–150.
Ding, S.F., Wei, W., Zhao, G.C., 2007. Electrochem. Commun. 9, 2202–2206.
Elkaoutit, M., Naranjo-Rodriguez, I., Dominguez, M., Hernandez-Artiga, M.P., Bellida-Milla, D., de Cisneros, J., 2008. Electrochim. Acta 53, 7131–7137.
Feng, X.D., Sayle, D.C., Wang, Z.L., Paras, M.S., Santora, B., Sutorik, A.C., Sayle, T.X.T., Yang, Y., Ding, Y., Wang, X.D., Her, Y.S., 2006. Science 312, 1504–1508.
Guo, S.J., Wang, E.K., 2007. Anal. Chim. Acta 598, 181–192.
Huang, H., Hu, N.F., Zeng, Y.H., Zhou, G., 2002. Anal. Biochem. 308, 141–151.
Kamin, R.A., Willson, G.S., 1980. Anal. Chem. 52, 1198.
Kim, S.K., Yoon, P.W., Paik, U., Katoh, T., Park, J.G., 2004. Jpn. J. Appl. Phys. Part 1 Regul. Papers Short Notes & Rev. Papers 43 (11A), 7427–7433.
Kristinsson, H.G., 2002. J. Agric. Food Chem. 50, 7669–7676.
Li, J.W., Liu, L.H., Xiao, F., Gui, Z., Yan, R., Zhao, F.Q., Hu, L., Zeng, B.Z., 2008. J. Electroanal. Chem. 613, 51–57.
Li, Q.W., Luo, G.A., Feng, J., 2001. Electroanalysis 13, 359–363.
Liu, A.H., Wei, M.D., Honma, I., Zhou, H.S., 2005. Anal. Chem. 77, 8068–8074.
Liu, G.Z., Paddon-Row, M.N., Gooding, J.J., 2007. Electrochem. Commun. 9, 2218–2223.
Liu, H., Hu, N.F., 2003. Anal. Chim. Acta 481, 91–99.
Liu, Y., Lei, J.P., Ju, H.X., 2008. Talanta 74, 965–970.
Murray, R.W., 1984. In: Bard, A.J. (Ed.), Electroanalytical Chemistry. Marcel Dekker, New York, pp. 191–368.
Schubert, D., Dargusch, R., Raitano, J., Chan, S.W., 2006. Biochem. Biophys. Res. Commun. 342, 86–91.
Si, R., Zhang, Y.W., Li, S.J., Lin, B.X., Yan, C.H., 2004. J. Phys. Chem. B 108, 12481–12488.
Si, R., Zhang, Y.W., You, L.P., Yan, C.H., 2005. Angew. Chem., Int. Ed. 44, 3256.
Song, Y.H., Wang, L., Ren, C.B., Zhu, G.Y., Li, Z., 2006. Sens. Actuators. B Chem. 114, 1001–1006.
Sun, D., Cai, C., Li, X., Xing, W., Lu, T., 2004. J. Electroanal. Chem. 566, 415.
Tarnuzzer, R.W., Colon, J., Patil, S., Seal, S., 2005. Nanoletters 5, 2573–2577.
Tsai, Y.Y., Oca-Cossio, J., Agering, K., Simpson, N.E., Atkinson, M.A., Wasserfall, C.H., Constantinidis, I., Sigmund, W., 2007. Nanomedicine 2 (3), 325–332.
Wang, S.F., Chen, T., Zhang, Z.L., Shen, X.C., Lu, Z.X., Pang, D.W., Wong, K.Y., 2005. Langmuir 21 (20), 9260–9266.
Wu, F., Xu, J., Tian, Y., Hu, Z., Wang, L., Xian, Y., Jin, L., 2008. Biosens. Bioelectron. 24, 198–203.
Xi, F.N., Liu, L.J., Wu, Q., Lin, X.F., 2008. Biosens. Bioelectron. 24 (1), 29–34.
Xu, J.M., Li, W., Yin, Q.F., Zhong, H., Zhu, Y.L., Jin, L.T., 2007a. J. Colloid Interface Sci. 315, 170–176.
Xu, Q., Mao, C., Liu, N.N., Zhu, J.J., Sheng, J., 2006. Biosens. Bioelectron. 22, 768–773.
Xu, S.Y., Peng, B., Han, X.Z., 2007b. Biosens. Bioelectron. 22 (8), 1807–1810.
Yan, R., Zhao, F.Q., Li, J.W., Mao, F., Fan, S.S., Zeng, B.Z., 2007. Electrochim. Acta 52 (26), 7425–7431.

Yang, Z.Q., Zhou, K.B., Liu, X.W., Tian, Q., Lu, D.Y., Yang, S., 2007. Nanotechnology 18 (18).
Zhang, H.L., Lai, G.S., Han, D.Y., Yu, A.M., 2008. Anal. Bioanal. Chem. 390 (3), 971–977.
Zhao, X.J., Mai, Z.B., Kang, X.H., Zou, X.Y., 2008. Biosens. Bioelectron. 23 (7), 1032–1038.
Zhou, K.B., Yang, Z.Q., Yang, S., 2007. Chem. Mater. 19, 1215–1217.
Zhu, L.D., Yang, R.L., Zhai, J.G., Tian, C.Y., 2007. Biosens. Bioelectron. 23, 528–535.
Zhu, Y.C., Cheng, G.J., Dong, S.J., 2002. Biophys. Chem. 97 (2–3), 129–138.
Zong, S.Z., Cao, Y., Zhou, Y.M., Ju, H.X., 2006. Langmuir 22, 8915.